Journal of Distributed Computing and Systems(JDCS), Vol. 4, Issue 2, 2021, Pages 83-91

# Improve The Automatic Detection of Welding Defects in Steel Structures Using Fuzzy Clustering Algorithm

Hasan N. Bairmani[1], Mojtaba B Taghadosi[2], Ali H. Jawdhari[3], Ghassan Fadhil Smaisim[4], Husam A. Al-Hameed[5]
[1]*Faculty of Electrical Department, Track Mechatronic, Imam Reza International University Mashhad, Iran.*
[2]*Karbala Refinery Oil Project.*
[3]*General Company for Electrical Energy Production Basra, Iraq.*
[4]*Department of Mechanical Engineering, Faculty of Engineering, University of Kufa, Iraq.*
[5]*General Company for The Manufacture of Cars and Equipment Babylon, Iraq.*

**Article History:**

Received: 29 November 2021
Received in revised form: 6 February 2022
Accepted: 15 February 2022
Available online: 17 March 2022

## Abstract

The metal-to-metal connection uses a special welding process, the quality control of which is so important that today the visual control method of destructive analysis has almost replaced the automatic non-destructive detection of welding defects. Among non-destructive methods, this particular method is more comprehensive due to the cheapness of radiography compared to other non-destructive methods and the simplicity of radiographic image analysis. However, the diagnosis of human welding defects may be related to errors due to the low quality of radiographic images. Therefore, today's radiographic images are analyzed by computer and automated image processing methods. In this work, a clustering method has been used to detect welding defects. The process is to first remove the negative effects such as noise in the image through preprocessing, improve the image quality, and then implement the fuzzy C-means (FCM) algorithm to identify welding defects. In this work, the independent variable is the number of clusters in the fuzzy clustering, and it has been shown that the accuracy of detecting defects in welding images increases as the number of clusters increases. Furthermore, based on the obtained results, the average accuracy of the method for small cracks, large cracks, and void defects is 92.01%, 94.67%, and 99.92%, respectively.

**Keywords:** Control System, Matlab, Welding Defects, Fuzzy Clustering Algorithm.

## I. INTRODUCTION

With the development of various welding process applications and their entry into the industry, this process has been proposed as the most important process for joining metal parts and has been considered for various applications like air conditioning and heating systems due to its main advantages such as speed and efficiency [1-3], rotating equipment [4-5], intelligent systems [6-7] and many types of electronic equipment [8-9], which are used in different industries including aerospace [10], solar energy [11-12], fuel cell [13-14], electrical [15-16], nanometer [17-18], automotive [19-20] applications.

Since welding quality control is a very important issue, in addition to visual inspection methods and destructive analysis, non-destructive testing (NDT) is also considered by the public in welding control. Due to increasing success, non-destructive methods have found their way into various industries including foundry and non-metallic industries. Liquid penetrant testing (LPT), magnetic particle testing (MPT), and eddy current testing (EDT) are used to identify surface defects in welds, and industrial radiography and ultrasonic testing are used to identify deep defects in welds [21].

Since X-ray image analysis is simpler and less expensive than ultrasonic inspection, and X-ray is cheaper and more durable than ultrasonic inspection, this method has received more attention and is more widely used in the industry. In film-based radiographic methods, the results are subject to human error based on the quality and clarity of the film and depending on the welding position, but in newer methods using computer-based image processing and machine

*Corresponding Author: Ghassan.smaisim@uokufa.edu.iq

vision, high-quality and high-resolution Films can be produced and welding defects identified in the shortest time and in the most accurate way [22].

Due to the importance and role of NDT in ensuring proper weld performance, these tests have been extensively studied and compared by many researchers in the field. The most common NDT tests are radiographic imaging, ultrasound, and magnetic resonance imaging. Gamma radiographic testing (GRT) is one of the common and important applications of radioisotopes in the industry [23-25].

GRT is used in the industry to evaluate welding performance by radiographic images. The advantages of gamma imaging compared to other methods are comprehensive performance, non-disruption, high speed, and low cost. Gamma testing uses gamma-ray isotopes to check for weld defects. An operator or computer is used to interpret these images. For automatic interpretation, images are first stored digitally, then image quality is improved by preprocessing algorithms, and finally, methods related to defect detection are applied. Various methods can be used to identify defects in images [26-29].

The method proposed by Suhaila Abd Halim et al. Focus on pinpointing weld areas and defect areas with precision. The algorithm uses non-destructive testing methods to determine weld defects. Any defect that prevents successful welding is called a welding defect. Edge extraction of segmented weld defects to analyze defects. In this approach, welding defect detection can be improved by detecting welding defects and examining geometric features [30].

Another approach was proposed by H. Kasban et al., who extracted features from radiographic images to detect welding defects. In this method, the image is first converted into a one-dimensional signal. In the next step, for each transform, the common Mel-frequency coefficient cepstral and polynomial coefficients of the signal are obtained. Then, to extract features and compare them with each other, they obtained wavelet and discrete Fourier transforms. 16 radiographs including Gaussian noise, speckle noise and Poisson noise and 72 weld defects have been used to evaluate the effectiveness of the method. According to the research results, the method can be used to automatically detect welding defects in radiographic images as well as in noisy environments [31].

In [32], the authors used geometric methods to find and classify welding defects in radiographs. First, for each segmented part, a set of 41 descriptors with the same texture patterns and geometric features is obtained, and this set is then used as the input to the classifier. The classifier uses image specifications with welding defects to learn how to classify each object in the class. Validated results using three methods of support vector machines, neural networks and k-nearest neighbors are examined.

Among smoothing and denoising strategies, non-linear strategies were found to convey more satisfactory results compared to direct strategies. Some nonlinear methods using anisotropic diffusion filters (ADF), non-local means (NLM), fourth-order partial differential equations (PDE), range and domain filter grouping, nonlinear Gaussian filters and bilateral filters and their Extended filters for triangles [33-34], and are well known. In this paper, an anisotropic diffusion-based scheme is proposed to solve the problem of the deformed position of welds in noisy images. Perona and Malik were the first to use the anisotropic diffusion equation for image smoothing and edge finding. This classic strategy is called the P-M model [35], which enhances edge detection, image upscaling, image smoothing, image reconstruction, and intra-image feature partitioning. In [36, 37], two methods were proposed, followed by the P-M model, which has convinced many to date. Carter et al. [36] proposed a scheme that uses a Gaussian filter for pre-denoising before each iteration of the spread function. This scheme can effectively reduce noise; therefore, determining a reasonable value for the σ parameter of the Gaussian filter remains a problem.

Rudin et al. [37] proposed a nonlinear Total Variation (TV) strategy. This scheme uses only gradients to have a better effect on the stairs. For a long time later, some modified anisotropic diffusion (AD) models with different schemes have been drawn closer for digital image processing. The modified AD models can be classified into two categories according to denoising processing and edge protection. On denoising strategies utilizing neighborhood data for propagation preparation, Tsai and Chao et al. Several anisotropic diffusion-based methods [38–43] have been proposed for noise removal and defect detection in sputtered glass, astronomical images, lean thin-film transistor images, solar wafers, and surface images. Tsai and Chao [38] defined an anisotropic diffusion (TCAD) strategy to detect defects in sputtered glass substrates with uneven texture. This strategy adaptively adjusts the importance of edge gradients using a non-negative decreasing function with a hardening gradient threshold as the diffusion coefficient. Chao and Tsai [39] encouraged to proposal an enhanced anisotropic diffusion strategy called CTAD. To remove noisy stars from nebula images, the strategy incorporates nearby grayscale fluctuation data into the propagation coefficient work. Another adaptation of the diffusion model [40] called CTAD-TFT effectively sharpens and smoothes low-contrast surface images, especially in glass substrates for lean thin-film transistor-liquid gemstones, used in classical PM. Weighted sharpening spread function smoothing process model.

In the subsequent sections of this paper, the proposed method is reviewed and numerical results are obtained from the implementation of the proposed method.

## II. FUZZY C-MEANS CLUSTERING ALGORITHM

In 1965, Lotfizadeh proposed fuzzy set theory, which became the basis of fuzzy clustering. Each cluster in fuzzy clustering has a set of members, and each member can belong to several other clusters with different membership ratios [41]. Fuzzy clustering of sets S to v clusters is defined by v membership function Uj. The following relationships are properties of membership functions:

$$U_j: S \to [0.1]\ j = 1.2. \ldots . v \quad (1)$$

$$\sum_{j=1}^{v} U_j\,(x_i) = 1\ i = 1.2. \ldots . l \quad (2)$$

$$0 < \sum_{i=1}^{l} U_j\,(x_i) < l\ j = 1.2. \ldots . v \quad (3)$$

In the above relationship, Uj is the membership function. In this type of clustering, each xi vector can be assigned to each cluster with membership in the interval [0,1] specified by the membership function Uj [42].

In the fuzzy clustering algorithm, like the K-mean algorithm, it is necessary to preliminarily determine the number of clusters. In this method, the objective function is defined as follows.

$$J_m(U,Z;X) = \sum_{i=1}^{c}\sum_{k=1}^{n} u_{ik}^{m}\, D_{ik}^{2} = \sum_{i=1}^{c}\sum_{k=1}^{n} u_{ik}^{m}\, \|x_k - v_i\|^2 \quad (4)$$

Where $D_{ik}^2$ is the distance between the data $x_k$ and the center of the cluster $\boldsymbol{i}$. m ∈ [0, ∞) also determines the fuzzy value of the algorithm (usually m = 2). If m→1, the clustering will go into hard clustering, if m→∞, the clustering will go into fuzzy clustering. The membership degree of each data to each cluster is determined by the membership matrix $U = [u_{ik}]_{c\times n} = (u_1.u_1.\ldots u_l)$ where c represents the number of clusters and n represents the number of clusters data. The values of matrix U can be between 0 and 1, and the values of each column must sum to 1[43].

$$\sum_{i=1}^{c} u_{ik} = 1\ .\forall\ k = 1.2. \ldots . n \quad (5)$$

Using Equation (8) as well as minimizing the objective function, the following equations are obtained:

$$u_{ik} = \frac{1}{\sum_{j=1}^{c}\left(\frac{d_{ik}}{d_{jk}}\right)^{2/(m-1)}} \quad (6)$$

$$v_i = \frac{\sum_{k=1}^{n} u_{ik}^{m} x_k}{\sum_{k=1}^{n} u_{ik}^{m}} \quad (7)$$

FCM includes the following steps:

1- Initialize parameters c, m and U.

2- Randomly select primary cluster centers.

3- Determine the center (vi) of the new cluster.

4- Determine the membership matrix of the clusters from the clusters computed in the second step.

5- If the condition $\|U_{l+1} - U_l\| < \in$ holds, the algorithm terminates.

In this algorithm, the determination of convergence and data training is also unsupervised. Disadvantages of this algorithm include long computation time and sensitivity to the selection of primary cluster centers [44].

## III. PROPOSED METHOD

Our proposed method consists of four steps; 1- capturing digital radiographs, 2- improving images (preprocessing stage), 3- segmenting images, and finally 4- finding welding defects. Each stage consists of multiple processes, each of which separately provides input to the next stage by performing its tasks correctly. Digital radiographs can be provided by digital cameras or scanners. During the recording of these photos, there may be damaging environmental effects on the quality of the photos, and noise may appear in the photos. First, the task of the image improvement part is to bring the image quality to the desired level and prepare it for the next step. Then, in the segmentation stage, try to identify large weld areas and separate them from the image background. Finally, the images are clustered by the FCM algorithm to find candidate defect regions, and after the images are completely classified, these regions are identified and compared with the actual defect regions to obtain the accuracy of the proposed method. The flowchart of the proposed method is shown in Fig. (1). In the following, each stage of the work is explained independently [45].

### *A.Digital radiographs*

Digital radiographs can be provided by digital cameras or scanners, which will have good quality images if their imaging clarity is 2400 dpi.

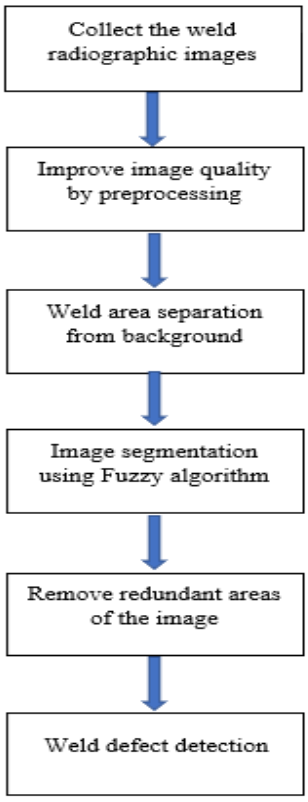


**Fig. 1.** Flowchart of the proposed method.

*B. Pre-processing*

Some of the problems with detecting welding defects through image processing are:

• Low image brightness
• Gray focus, low image contrast
• Images with blurred edges
• Large noise in the image

Due to the above problems, the following methods can be used in the proposed algorithm:

*A. Histogram Equalization*

One of the uses of a histogram is to increase the contrast of low-contrast images. When the image contrast is low, it means that the difference between the minimum and maximum brightness of the image is small. Adjust the histogram to increase the contrast of the input image as much as possible. Figure (2) shows the image before and after histogram equalization:

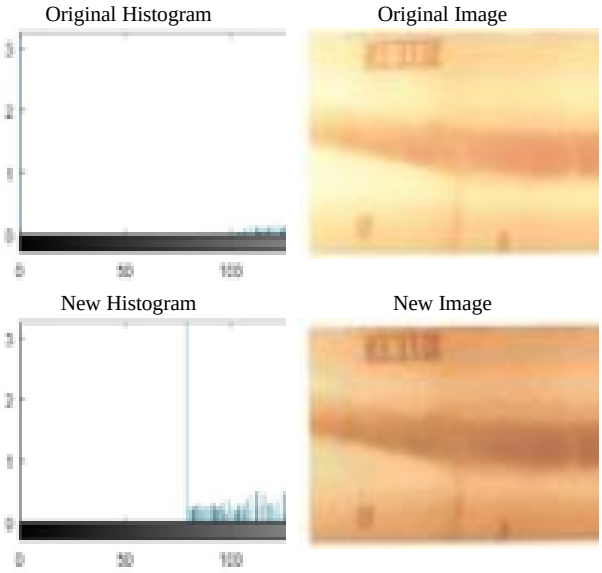


**Fig. 2.** Histogram Equalization in the images to improve the quality [46]

In this work, a histogram equalization operation is used to improve the contrast of the image. This improves the quality of the input image and leads to more accurate noise removal and region separation [46].

B. NOISE REMOVAL FILTERS

In this step, image noise is reduced by using various filters. Filters suitable for this purpose are the average filter and the medium filter. An intermediate filter is a nonlinear low-pass filter used to remove speckle noise from an image. This filter removes noise without removing or destroying pixels. This filter is commonly used to remove noise in radiographic images. In this work, a medium filter is used to remove salt and pepper noise [47]. In this work, a 3*3 mask is used to filter the image.

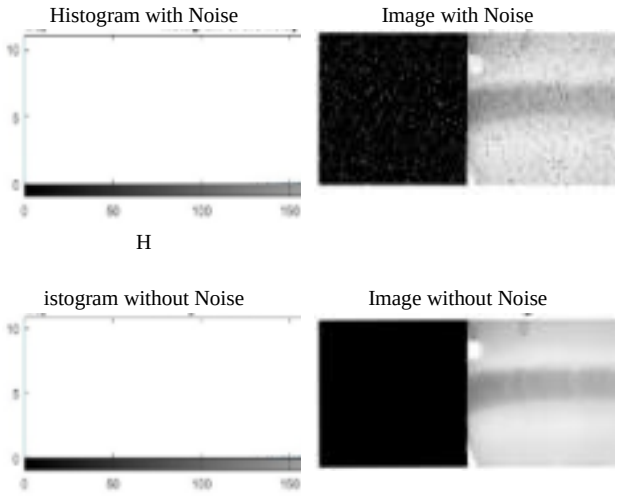


**Fig. 3.** Noise removal from the image using the medium filter [47]

## IV. WELD AREA SEPARATION

Images taken from welds include additional information such as length, item characteristics, and weld number. It is better to separate the weld area in the image from other additional information and use it as input for the main processing. Figure (4) also shows the separation of the redundant area from the welded area. Separating these areas is a very important operation. In this work, a threshold operation has been used to separate these regions.

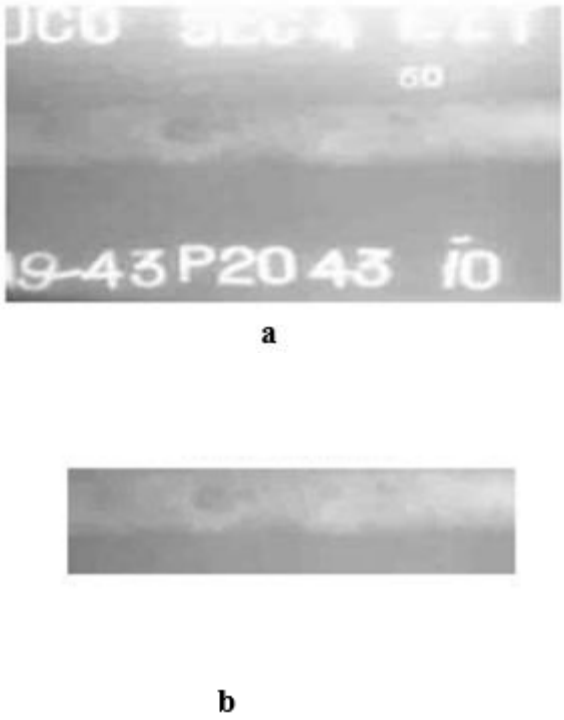

**Fig. 4.** Separation of excess areas from the weld area: a. original image, b. weld area.[46]

## V. FIND THE DEFECT AREA USING IMAGE SEGMENTATION WITH FCM

The regions that need to be segmented and extracted are the only ones that need to be welded, separating irrelevant information from the image. For this, segmentation methods commonly used in radiographic images are used, i.e. a set of filters such as Kirsch, bridge, smoothing or Prewi to find important information (welding defects) in the image pixels. At this step, the segmentation can be performed using a fuzzy clustering algorithm. For example, Figure (5) shows the segmentation of a welding image using a blurring algorithm. The image is segmented for many different regions. The more regions, the better the segmentation quality.

To extract weld crack regions, FCM considers segmenting the image and selects the darkest clusters as crack regions. Then, with the help of attributes such as size, non-defective areas of the weld are identified and removed.

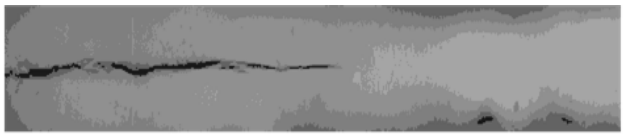

**Fig. 5.** Segmentation of a welding radiograph [47]

## VI. SIMULATION RESULTS

In this section, simulation results of the proposed method for evaluating system performance are presented. In the following, first a description of the data collected and their classification into several different groups according to the type of cracks and weld defects, and then the output of each step of the proposed method is explained in order to better understand the different groups of systems Images are given. Finally, the accuracy of the method on different types of data is given.

### *A. Data*

The input data of the proposed method is a collection of radiographic images, which are divided into 3 different categories [47], which are: 1- Data with cavity defects. 2- Data with large cracks 3- Data with small cracks. To simulate the real environment, the images have different qualities and different noises, examples of each category can be seen in Figure (6).

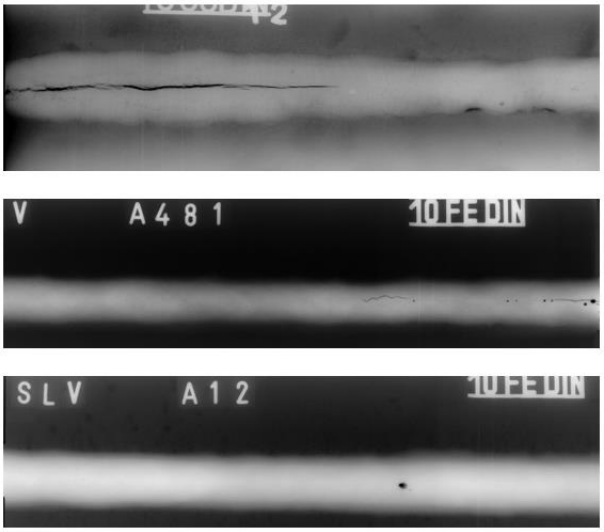


**Fig. 6.** Preliminary images, a. Large cracks, b. Small cracks, c. Cavities

Due to the efficiency of the proposed method in this work, multiple images use different features. In Figure (7) you can see an example of images used to evaluate the proposed method. The range of images used to evaluate the proposed method includes cracks and voids with various sizes and

shapes. Furthermore, the background of the image has various shapes, which can indicate the accuracy of the proposed method in the initial separation of the welding area from the background image.

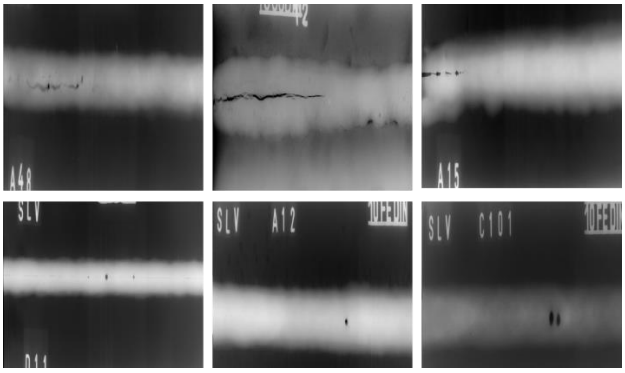

**Fig. 7.** The different type of images used to evaluate the proposed method, including cracks and cavities with various dimensions and shapes

*B. Implementation*

After collecting the data and classifying them into different groups, execute the proposed algorithm described in the previous section.

1- In the first step, load the real image obtained from the database.

2- Next, the image is split into 0 and 1 parts. This means that all pixels below a threshold level become 0, and pixels above that threshold level become 1. In this way, the whole image is divided into two parts. Figure (8.b) shows the binary and segmented main image.

3- Since the purpose is to identify the weld area, the area around the metal should be removed and only the main area known as the weld area should be identified. To this end, at this stage, the largest area is selected as the welding area, and the rest are zero. Figure (8.c) shows the binary image after separation of the weld area.

4- In this step, the weld area is cut on the master image and the type of weld cracks are divided into the desired area, depending on whether they are in the center of the area or at the top and bottom of the area. Figure (8.d) shows a large crack cut in the welded area on the original image.

5- Then perform the main phase of the work, which is clustering using the FCM algorithm. In this way, the parameters of the FCM algorithm are first determined, and then the algorithm is executed to divide the image into several clusters. The desired image is then divided into different parts based on these clusters, and the final image clusters are obtained according to the FCM algorithm. Figure (8.e) also shows the initial image segmented by the FCM algorithm.

6- In the last step, extract the area related to the weld crack from the entire desired area. In this step, the weld crack region is extracted, and considering the image segmented with FCM, the darkest cluster is selected as the crack region. Figure (8.f) shows the extraction of defect regions using the FCM algorithm.

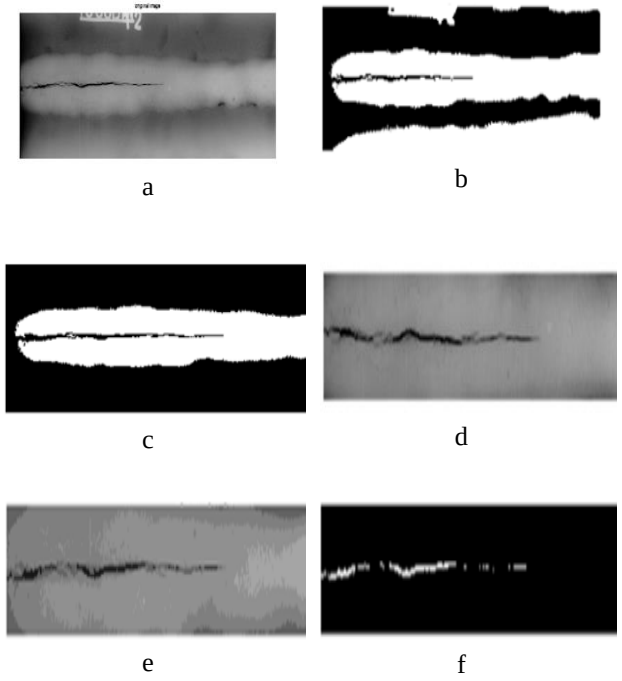


**Fig. 8.** Different steps of the proposed method in images with large cracks: original image, b. Binary and segmented raw images, c. Binary image after separation of welding regions, d. Cut out the welded area in the original image, eg. Initial image for FCM segmentation, f. Defect regions are extracted using the FCM algorithm.

*C. Evaluate the proposed method*

Finally, to evaluate the proposed algorithm, the correct areas of the weld cracks in the image, called Ground Truth, are first obtained manually, then these Ground Truth areas are compared with the areas obtained using the FCM algorithm, and the areas are correctly detected with the FCM algorithm according to the number of, the accuracy of the proposed method is obtained.


**Fig. 9.** Comparison of defect areas for large cracks in a. Original images b. Using the proposed method

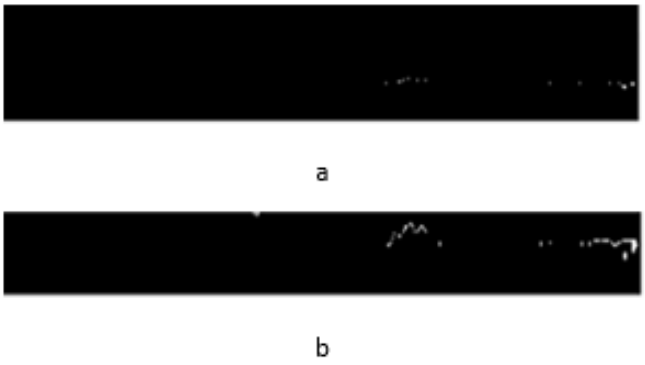


**Fig. 10.** Comparison of defect areas for small cracks in a. Original images b. Using the proposed method

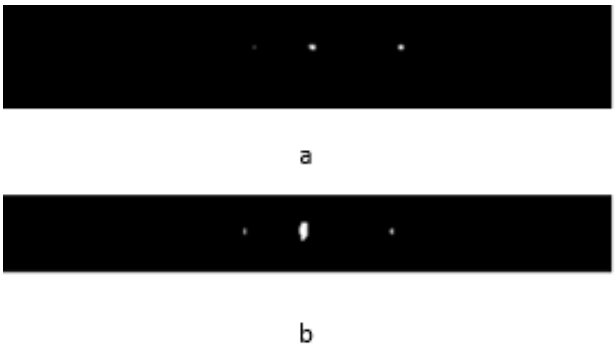


**Fig. 11.** Comparison of defect areas for cavities in a. Original images b. Using the proposed method

The accuracy of weld defect detection in this system is measured by using the correct length and area detected by the algorithm. The average accuracies for all defects of large and small cracks and voids are listed in Table (1).
The results in Table 1 show that the proposed algorithm has an average accuracy of 92.01%, 94.67% and 99.92% for weld defect detection of small cracks, large cracks and voids, respectively.
The results of this study show that the best performance of the algorithm is on void defects, while the weakest performance of the algorithm is on small cracks.

**TABLE 1.** Mean accuracy for all type of defects detection

| Mean Accuracy (%) | Type of defect |
|---|---|
| 92.01% | Small cracks |
| 94.67% | Large cracks |
| 99.92% | Cavities |

It should be noted that since the FCM algorithm sometimes fails to find cluster heads in local optimization, to avoid this problem, the results are recorded after 50 iterations per image.

## VII. CONCLUSIONS

Automated methods are widely used to interpret and determine weld quality in radiographic images because of their simplicity, speed, and low cost. Numerous algorithms have been proposed to automatically detect welding defects, which are implemented with the help of machine vision techniques and digital image processing. In this work, an automatic method based on fuzzy clustering is used to detect regions related to welding defects. The FCM algorithm is a very effective method in digital image processing, and the algorithm also achieves high precision in the segmentation and detection of welding defects.

**TABLE 2.** Description of Parameters

| **Nomenclature** | | | |
|---|---|---|---|
| U | Total number of Matrix | NLM | Non-Local Means |
| $v$ | Clusters | PDE | Fourth Order Partial Differential Equation |
| e | Rib Height (m) | P–M Model | Perona and Malik Model |
| c | indicates the number of clusters | FCM | Fuzzy C-Means Algorithm |
| u | Matrix | NDT | Non-Destructive Test |
| x , y, z | Cartesian Coordinate in Horizontal, Vertical, Depth Direction | LPT | Liquid Penetrant Testing |
| i | Number of rows | MPT | Magnetic Particle Test |
| j | Number of column | EDT | Eddy Current Testing |
| t | Total | GRT | Gamma Radiography Test |
| AD | Anisotropic Diffusion | TCAD | Tsai and Chao an anisotropic diffusion strategy |
| ADF | Anisotropic Diffusion Filter | | |

## VIII. REFERENCES

[1] *Smaisim G.F.'' Investigation on heat transfer augmentation using continuous and broken ribs on a plate of heat exchanger'', International Journal of Energy and Environment, 9(3), 2018 pp.211-232.*

[2] *You D.Y., Gao X.D., Katayama S. Review of laser welding monitoring. Sci. Technol. Weld. Join. 2013;19:181–201. doi: 10.1179/1362171813Y.0000000180.*

[3] *M. Jasem, N., Fadhil. Smaisim G., & H. Mohammed, H. (2009). Experimental Study of the Effect Bed Density On Heat Transfer Coefficents in Towers with Gas Solid Circulating Fluidized Bed. Al-Qadisiyah Journal for Engineering Sciences, 2(3).*

[4] *Smaisim, G. F.; Fatla, O. M.H.; Medina, A. Valera; Rageb, A. and Syred, N.(2016, Jan), Investigation of Heat Transfer and Fluid Mechanics across a Heated Rotating Circular Cylinder in Crossflow, AIAA*

*Science and Technology Forum and Exposition, San Diego, U.S.A. 4-8.*

[5] *Smaisim, G. F., Fatla, O. M.; Medina, A. Valera; Rageb A. and Syred N., (2016). Experimental and Theoretical Investigation of the Effect of Rotating Circular Cylinder Speed on the Lift and Drag Forces", International Journal of Energy and Environment, Vol. 7, Issue 1, PP.23-36.*

[6] *Ahmadi, M. R., Hussien, N. A., Smaisim, G. F., & Falai, N. M. (2019). A Survey of Smart Control System for Poultry Farm Techniques. In Proc of the International Conference on Distributed Computing and High Performance Computing (DCHPC2018) (pp. 25-27).*

[7] *N. Ali Hussien, A. M Alaidib, T. Ali Alquraish, G.F. Smaisim (2019) Improvement the Route Discovery Mechanism of Dynamic Source Routing Protocol in MANET. International Conference on Distributed Computing and High Performance Computing (DCHPC2018).*

[8] *Fatla, O. M.; Smaisim G.F.; Medina, A. Valera; Rageb A. and Syred N., (2015, June). Experimental and Numerical Investigation of Heat Transfer and Fluid Mechanics across a Rotating Circular Cylinder Dissipating Uniform Heat Flux by Crossflow, 10th Pacific Symposium on Flow Visualization and Image Processing Naples, Italy.*

[9] *Oh, Sang-jin, Min-jae Jung, Chaeog Lim, and Sung-chul Shin. 2020. "Automatic Detection of Welding Defects Using Faster R-CNN" Applied Sciences 10, no. 23: 8629. https://doi.org/10.3390/app10238629*

[10] *Smaisim, G. F., (2017). Enhancement Heat Transfer of Cu-Water Nanofluids with Thermophysical Properties Modeling by Artificial Neural Network, Journal of Babylon University, Engineering Sciences, No. (5), Vol. (25).*

[11] *Smaisim, G. F. (2010). The Effects of Cylinder at the Leading Edge of Airfoil NACA 0012 on the Boundary Layer Separation. Kufa Journal of Engineering, 1(2). Retrieved from https://journal.uokufa.edu.iq/index.php/kje/article/view/1297*

[12] *Ali K. Al-Abadi, Ahmed F. Kridi, Ghassan Fadhil Smaisim. ''Comparison Between Simulated and Calculated Power of the Solar Chimney with Black Concrete Base using Ansys Program'', Al-Qadisiya Journal For Engineering Sciences 3(3) 2010.*

[13] *Al-Madhhachi H. and Ghassan F. Smaisim, Experimental and numerical investigations with environmental impacts of affordable square pyramid solar still Solar Energy 216 (2021) 303-314.*

[14] *Hinton G., Deng L., Yu D., Dahl G.E., Mohamed A.-R., Jaitly N., Senior A., Vanhoucke V., Nguyen P., Sainath T.N., et al. Deep Neural Networks for Acoustic Modeling in Speech Recognition: The Shared Views of Four Research Groups. IEEE Signal Process. Mag. 2012; 29:82–97. doi: 10.1109/MSP.2012.2205597.*

[15] *Stavridis J., Papacharalampopoulos A., Stavropoulos P. Quality assessment in laser welding: A critical review. Int. J. Adv. Manuf. Technol. 2017; 94:1825–1847. doi: 10.1007/s00170-017-0461-4.*

[16] *Purtonen T., Kalliosaari A., Salminen A. Monitoring and Adaptive Control of Laser Processes. Phys. Proc. 2014;56:1218–1231. doi: 10.1016/j.phpro.2014.08.038.*

[17] *Smaisim, G., M. Hassan, Z., and Muhammad Sadiq, M. (2017),''Analysing Shock Losses Throughout the Impeller of the Centrifugal Fan''. Al-Qadisiyah Journal for Engineering Sciences, 2(2), 335-352.*

[18] *Sallal, A.S.; Smaisim, G. F. and Thahab, S. M. (2021). Experimental and Numerical Investigation of Enhancement Heat Transfer from Fined Perforated Pipe Using Nano Fluid, Third International Scientific Conference of Engineering Sciences and Advances Technologies (IICESAT).*

[19] *Smaisim, G. F., (2017). Augmentation of Heat Transfer in Corrugated Tube Using Four-Start Spiral Wall" Al-Qadisiya Journal for Engineering Sciences, Vol .10, No. 4.*

[20] *Paszke A., Gross S., Massa F., Lerer A., Bradbury J., Chanan G., Killeen T., Lin Z., Gimelshein N., Antiga L., et al. PyTorch: An Imperative Style, High-Performance Deep Learning Library. In: Wallach H., Larochelle H., Beygelzimer A., Alché-Buc F.D., Fox E., Garnett R., editors. Advances in Neural Information Processing Systems 32. Curran Associates Inc.; New York, NY, USA: 2019. pp. 8024–8035.*

[21] *Practical Radiography, NDT20, TWI Ltd, UK, 1991.*

[22] *Payman Moallem, Ali Moallem, Crack Detection in Welding Radiography Images, in: Proceedings of the 2007 First International Conference on Technical Inspection and Nondestructive Testing, Tehran, Iran, 2007.*

[23] *Zahran, Al-Nualmy W. Recent development in ultrasonic techniques for rail-track inspection. In: Proceedings of NDT Conference, pp. 55-60, 2002.*

[24] *Ditchbum RJ, Burke SI (Scala CM). NDT of welds: state of the art. NDT E Int, pp.29 (2):111-7, 1996.*

[25] *Charles Hayes, The ABCs of nondestructive weld examination. Weld J, pp. 76(5):46-51, 1998.*

[26] *Wang G. Liao TW. identification of different types of welding defects in radiography images. NDT E Int, pp. 35:519-28, 2002.*

[27] *Da Silva Romeu R, Siqueira Marcia HS, Vieira de Souza Marcos Paulo, Rebello Joaidetildeo MA, Calawidehatb Luiz P. Estimated accuracy of*

*classification of defects detected in welded joints by radiography tests. NDT E Int, pp.38:335-43, 2005.*

*[28] Saravanan T, Bagavathiappan S, Philip J, Jayakumar T, Raj B. Segmentation of defects from radiography images by the histogram concavity threshold method. Insight, pp.49 (10):578- 84, 2007.*

*[29] Silva RR, Mary D. State-of-the-art of weld seam inspection by radiography testing: Part I: image processing. Mater Eval, pp.65 (6):643-7, 2007.*

*[30] Suhaila Abd Halim, Normi Abd Hadi, Arsmah Ibrahim, Yupiter HP Manurung, " The Geometrical Feature of Weld Defect in Assessing Digital Radiographic Image", Imaging Systems and Techniques (IST), 2011 IEEE International Conference on, pp. 189 – 193, 2011.*

*[31] Kasban H, Zahran O, Arafa H, El-Kordy M, Elaraby Sayed MS, Abd El-Samie FE. Welding defect detection from radiographic image using cepstral approach. NDT E Int, pp.226–31, 2011.*

*[32] I. Valavanis and D. Kosmopoulos, "Multiclass defect detection and classification in weld radiographic images using geometric and texture features," Expert Systems with Applications, vol. 37, pp. 7606-7614, 2010.*

*[33] J. Mohan, V. Krishnaveni, Y. Guo, A survey on the magnetic resonance image denoising methods, Biomed. Signal Process. Control 9 (2014) 56–69.*

*[34] C. Pal, A. Chakrabarti, R. Ghosh, A brief survey of recent edge-preserving smoothing algorithms on digital images, Proc. Comput. Sci. (2015) 1–40.*

*[35] P. Perona, J. Malik, Scale-space and edge detection using anisotropic diffusion, IEEE Trans. Pattern Anal. Mach. Intell. 12 (1990) 629–639.*

*[36] E. Catte, P.I. Lions, J.M. Morel, T. Coll, Image selective smoothing and edge detection by nonlinear diffusion, SIAM J. Numer. Anal. 29 (1992) 182–193.*

*[37] L.I. Rudin, S. Osher, E. Fatemi, Nonlinear total variation based noise removal algorithms, Physica D 60 (1992) 259–268.*

*[38] D.M. Tsai, S.M. Chao, An anisotropic diffusion-based defect detection for sputtered surfaces with inhomogeneous textures, Image Vis. Comput. 23 (2005) 325–338.*

*[39] S.M. Chao, D.M. Tsai, Astronomical image restoration using an improved anisotropic diffusion, Pattern Recognit. Lett. 27 (2006) 335–344.*

*[40] S.M. Chao, D.M. Tsai, An anisotropic diffusion-based defect detection for low contrast glass substrates, Image Vis. Comput. 26 (2008) 187–200.*

*[41] D.M. Tsai, C.C. Chang, S.M. Chao, Micro-crack inspection in heterogeneously textured solar wafers using anisotropic diffusion, Image Vis. Comput. 28 (2010) 491–501.*

*[42] S.M. Chao, D.M. Tsai, Anisotropic diffusion with generalized diffusion coefficient function for defect detection in low-contrast surface images, Pattern Recognit. 43 (2010) 1917–1931.*

*[43] S.M. Chao, D.M. Tsai, An improved anisotropic diffusion model for detail- and edge-preserving smoothing, Pattern Recognit. Lett. 31 (2010) 2012–2023.*

*[44] J.Tau, R. Gonzalez, "Pattern recognition principles", Addision Wesley, Reading, MA, 1974.*

*[45] J.C. Bezdek, "Pattern recognition with fuzzy objective function algorithms", Plenum Press. New York, 1981.*

*[46] R. Suganya, R. Shanthi, "Fuzzy c- means algorithm- a review", International Journal of Scientific and Research Publications, Vol. 2, 2012.*

*[47] A. Mahmoudi and F. Regragui, "Welding Defect Detection by Segmentation of Radiographic Images," CSIE '09 Proceedings of the 2009 WRI World Congress on Computer Science and Information Engineering, vol. 7, pp. 111-115, 2009.*

**How to cite:** H.N.Bairmani, M.B.Taghadosi, A.H.Jawdhari, Gh.F.Smaisim, H.A.Al-Hameed. Improve The Automatic Detection of Welding Defects in Steel Structures Using Fuzzy Clustering Algorithm, Journal of Distributed Computing and Systems(JDCS). Vol 4, Issue 2, Pages 83-91, 2021.